Journal of Civil Engineering, Science and Technology

Volume 17, Issue 1, April 2026, 19-29

DEVELOPMENT OF LIQUEFACTION HAZARD MAP FOR DINAJPUR MUNICIPALITY, BANGLADESH

Md. Mahabub Rahman[1*], Sonu Thakur[1], Syed Tanvir Ahmed[2] and Abu Sayed[3]

[1]Department of Civil Engineering, Hajee Mohammad Danesh Science and Technology University, Dinajpur, Bangladesh

[2]Department of Civil Engineering, California University Long Beach, California, USA

[3]Department of Civil Engineering, Pundra University of Science and Technology, Bogura, Bangladesh

Date received: 11/07/2024 **Date revised:** 31/08/2025 **Date accepted:** 19/09/2025 **Date published:** 30/04/2026

*Corresponding author's email: mmr.civil@hstu.ac.bd

DOI: 10.33736/jcest.7382.2026

Abstract — The word "earthquake" now denotes a global catastrophic natural event. Dinajpur Municipality is the most susceptible place to earthquake-induced liquefaction due to its geographical location. A crucial component of characterising a geotechnical site is determining the liquefaction resistance of loose saturated sand. The article employs a simplified approach reliant on the Standard Penetration Test's blow count (SPT-N) to evaluate the liquefaction risk triggered by the earthquake in Dinajpur Municipality. SPT data was collected at 78 sites within the study area. The potential risk of liquefaction was assessed at each site for several earthquake magnitudes, including 6, 6.5, 7, 7.5, 8, and 8.5, with a peak horizontal ground acceleration (PGA) of 0.20 g. The liquefaction risk was assessed using an estimated liquefaction potential index (LPI) for each location. The LPI values in the examined region varied from 8.6 to 15.9 for earthquakes of magnitude 8.5, indicating a risk level from moderate to extremely high. The LPI of locations was subsequently utilised to generate a risk map using geospatial approaches. The LPI was determined to be negligible in the middle and central-southern regions of the study area. The liquefaction susceptibility has been assessed as being significant in the northern and southwestern regions of the study sites. These results may be used to improve the subsurface conditions in the study area for the development of earthquake-resistant structures. The created risk map may serve as a significant signal for the Bangladesh government's catastrophe mitigation strategy.

2462-1382 / © 2026 The Author(s). Published by UNIMAS Publisher. This is an open access article under the CC BY-NC-SA 4.0 license (http://creativecommons.org/licenses/by-nc-sa/4.0/)..

***Keywords*:** SPT data, liquefaction, geospatial technique, kriging, hazard map

1.0 INTRODUCTION

Globally, infrastructure loss and damage are caused by long-term geotechnical risks brought on by earthquakes. One of the most damaging effects of an earthquake is liquefaction, which may seriously harm both human life and infrastructure [1]. Because of increased pore water pressure and reduced effective stress after an earthquake, granular soils undergo liquefaction, which is the process by which they change from a solid to a liquid state. Among other things, liquefaction has various effects on buildings, bridges, underground pipelines, and essential services [2-3]. Devastating historical occurrences have often struck Bangladesh, a nation that is prone to earthquakes [4]. The Dinajpur Municipality is in Bangladesh's northwest. Dinajpur's soil type is cohesionless (sandy), with a much higher ratio of sand to silt than clay, due to its location in the Terai basin. Numerous fault lines in this region make it vulnerable to earthquakes [5]. Because of the Jamuna fault, the Main Boundary Fault, and the active east-west running fault, Dinajpur, in northern India, is a seismically active region. Because of these factors, any earthquake in this area might cause significant harm to people and property, including educational institutions and other buildings [6]. The frequency, size, and severity of earthquakes have all risen recently, even though they are not a common issue in this area [7]. According to the seismic database, Bangladesh has seen more than 100 moderate-to-major earthquakes since 1900, with more than 65 of them occurring since 1960. This indicates a significant rise in earthquake frequency during the past three decades. These days, liquefaction brought on by earthquakes is a new and urgent worry.

Consequently, liquefaction risk has been evaluated for several seismically susceptible cities using simplified techniques. Determining this earthquake-caused geo-disaster has been the focus of several investigators. In this field, notable works include those by Mayya and Chatterjee [8], Singh [9], Kumar et al. [10], Hossain et al. [11], Ansari et al. [12], Subedi and Acharya [13], Nath et al. [14], Mase et al. [15], Rahman et al. [16], Sukkarak et al.

[17] and Hossain et al. [18]. Researchers produced susceptibility maps to facilitate the viewing of seismic sites [19]. A liquefaction hazard map is an essential product for identifying areas necessitating evaluations of liquefaction risks for the proposed project. Most liquefaction studies have focused on comparatively pure sands. Ground liquefaction has been examined in soils with grain sizes varying from very coarse sand to silty sand [20]. The simplified methods just assess the risk of liquefaction at designated sites. Drilling a borehole at every location in a community is almost unfeasible. Conversations focused on specific point results fail to encapsulate the whole context. The disaster mitigation policy must have a procedure for evaluating the severity of unsampled locations. A statistical analysis of the geographical distribution of discrete data is an effective method for generating a quantitative hazard map. Among the several statistical methodologies, geospatial analysis is the most pragmatic and is used across a broad spectrum of research. Kriging interpolation is an effective geostatistical technique that may precisely estimate values in unsampled locations [1]. This study is to evaluate the liquefaction susceptibility and create geo-hazard maps for several seismic events in Dinajpur Municipality, Bangladesh. Soil distribution maps for various strata are generated in ArcGIS, which is crucial for assessing soil liquefaction. This study utilises 78 borehole data from Dinajpur Municipality to create a soil distribution and liquefaction risk map.

1.1 Background

The most earthquake-prone region in Bangladesh is the northwest. The district of Dinajpur is located in the northwest of Bangladesh, close to the Dhubri Fault and the Himalayan frontal push. These tectonic belts in Bangladesh, Nepal, Myanmar, and north-eastern India have seen many historical earthquakes during the last 255 years (Figure 1) [15, 21]. With an epicentre around 250 kilometres from Dinajpur, the Great Indian Earthquake near Shillong, Assam, was one of the strongest earthquakes in history [22].

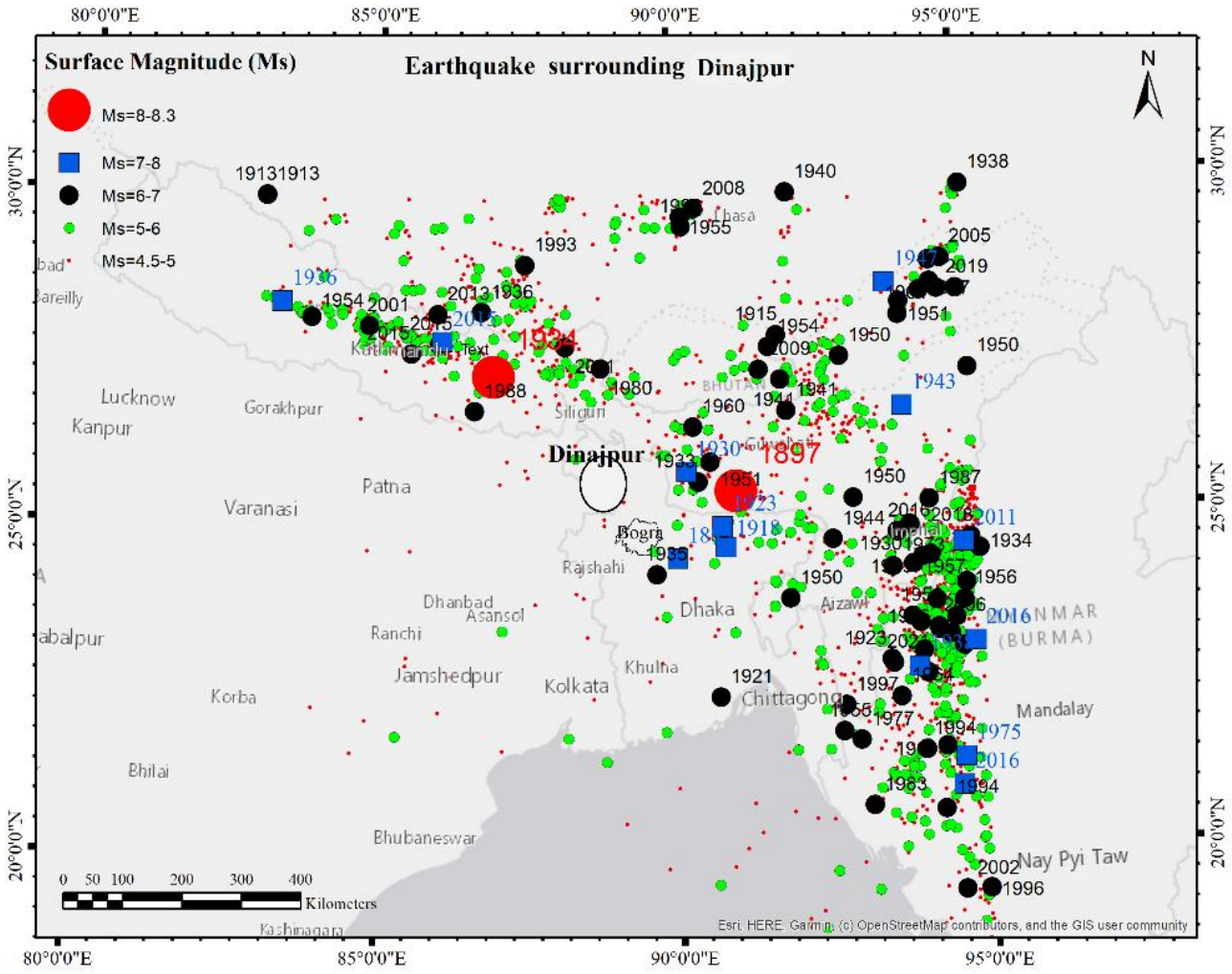


Figure 1 Earthquake location surrounding Bogura (1950-2023) [23]

The northwest of Bangladesh (Rangpur and Dinajpur) was damaged by the Shillong earthquake, which also destroyed infrastructure and railway connections, as well as masonry buildings throughout the nation [24]. In 1930, the Dhubri earthquake, which had a magnitude of M_w = 7.1, occurred in Bangladesh's Garo Hills region. Numerous buildings in Lalmonirhat, Rangpur, and Dinajpur have sustained damage. There has been concern recently about the frequency of various seismic events and the destruction they may inflict. This suggests that the region is experiencing a high level of seismic activity. The location of earthquakes in the study region is shown in Figure 1. Furthermore, many lakes and other bodies of water have been filled in to provide more residential and industrial space because of rapid industrialisation and population expansion. These areas are vulnerable to liquefaction in the event of an earthquake. A liquefaction risk assessment for Dinajpur Sadar became necessary because of these factors.

2.0 GEOLOGY AND SEISMOTECTONICS

Dinajpur Municipality is situated inside Dinajpur Sadar Upazila in the Dinajpur district of the Rangpur division. Presently, it is classified as a first-class municipality, including 12 wards and covering an area of 24.50 square kilometres. Figure 2 illustrates the geographical location of the study area.

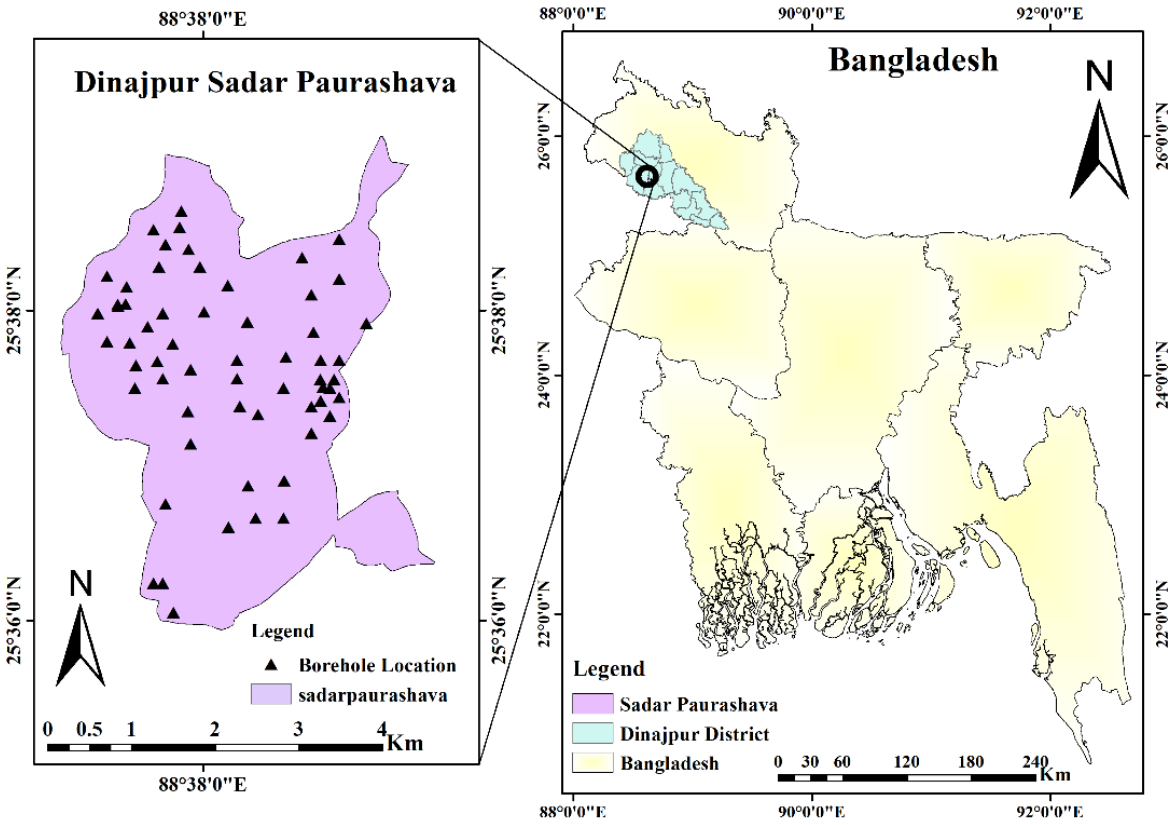


Figure 2 Geographical location of research area

The geology of the study area, characterised by ancient gravelly sand and clay residuum, is shown in Figure 3. The two significant active tectonic plates are responsible for the catastrophic and lethal earthquakes that have affected Bangladesh. The tectonic elements comprise the Arakan subduction-collision system to the east and the Himalayan system to the north. The main elements of the Himalayan system are the Himalayan Frontal Thrust and the Dauki Fault [25]. The study area is mostly comprised of Pleistocene alluvial deposits. Alluvial deposits consist of gravel, clay, silt, and sand. Figure 3 illustrates that ancient gravelly sand constitutes the predominant section of Dinajpur Municipality. Dinajpur was selected as the study area due to the prevalence of shallow focal earthquakes in and around the region, attributed to many faults, including the Bogra Fault, Sub-Dauki Fault, and Assam Fault.

3.0 DETERMINATION OF LPI

The LPI assesses liquefaction susceptibility and identifies possible damage and failure in locations prone to liquefaction. The LPI is calculated by combining the liquefaction safety factors throughout the whole soil profile depth of 0 to 20 m below the earth's surface at a specified site. Table 1 illustrates the liquefaction susceptibility quantified by the Liquefaction Potential Index (LPI), as assessed by Luna and Fros [26] and Iwasaki et al. [27]. The LPI and FS for liquefaction is determined by juxtaposing the cyclic stress ratio (CSR), indicative of seismic demand, with the cyclic resistance ratio (CRR), reflecting the soil's potential to withstand liquefaction. SPT report data is often used to evaluate a geological unit's liquefaction potential at depths of up to 40 feet below the surface. This study investigated the SPT number and other soil properties from 78 boreholes. Youd et al. [28] employed many boreholes in various geological units of Dinajpur Municipality to assess the safety factors against liquefaction. The LPI assessed for each SPT soil profile by empirical methods was used to generate a risk map for the research area. The soil database was obtained from the Local Government Engineering Department (LGED) and the Public Works Department (PWD) in Dinajpur, Bangladesh. The SPT-N levels of the soil varied between 2 and 38. The 78 borehole records indicate that the water table is located between 5.5 and 12 feet from the ground surface. The Dinajpur area is in a high seismic intensity zone, characterised by a zone coefficient of 0.20 g [29]. Historical data of significant earthquakes, together with the present distribution of seismic activity, substantiates the likelihood of a magnitude 6.5 or bigger earthquake occurring in or near Bangladesh, particularly near the city of Dinajpur. This study examines earthquake magnitudes ranging from 6 to 8.5 and a PGA of 0.20 g to determine the LPI for Dinajpur Municipality.

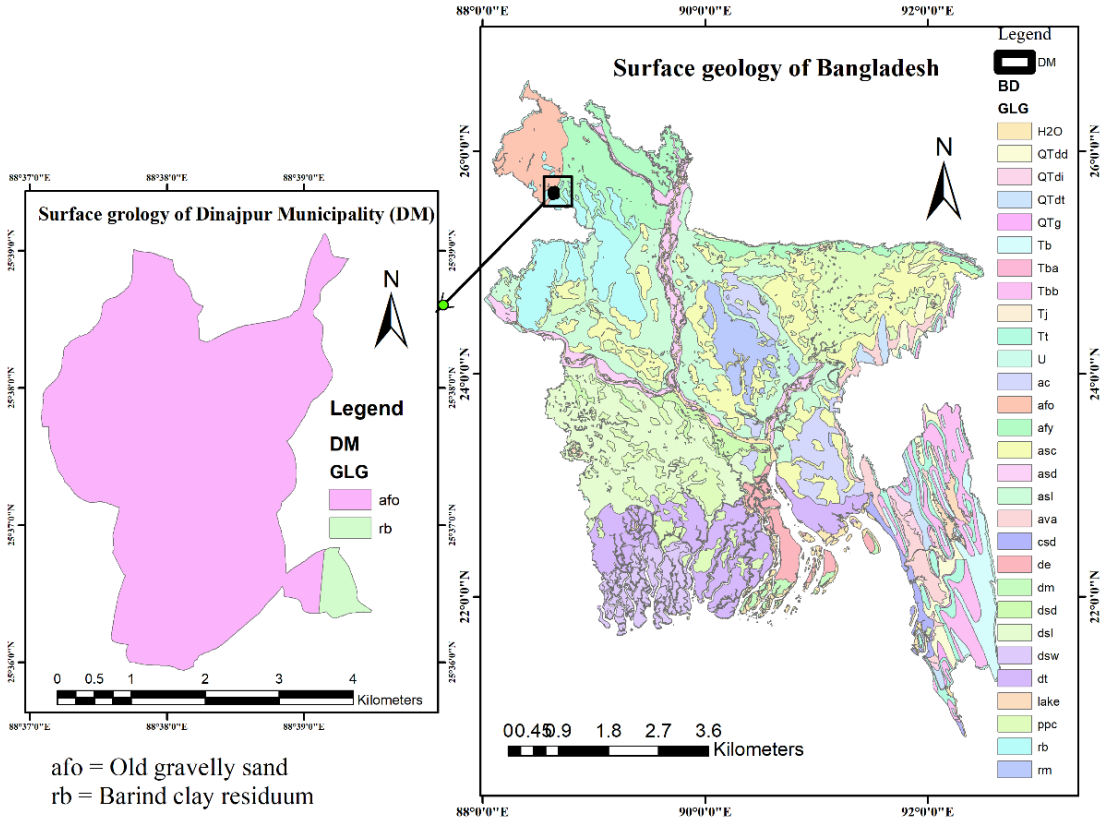


Figure 3 Dinajpur Sadar Upazila geological map

3.1. Simplified Approach

3.1.1. Idriss and Boulanger method

The LPI is evaluated for Dinajpur Municipality using a streamlined methodology from Idriss and Boulanger [30]. The following stages outline the procedure for assessing liquefaction risk:

Step 1:

The data gathered and utilised to estimate liquefaction susceptibility comprised groundwater elevation, SPT-N value, soil particle size distribution, and soil density.

Step 2:

Total vertical stress (σ_v) and effective vertical stress (σ_v') were computed for the various soil layers. Both stresses were considered. For each soil layer, the total vertical stress and effective vertical stress were calculated.

Step 3:

To determining the stress reduction factor (r_d), the Equations (1a-d) that follows may be used.

For, $z \leq 34$m,

$$r_d = \exp[\alpha(z) + \beta(z)M] \tag{1a}$$

Here,

$$\alpha(z) = -1.012 - 1.126 \sin[\frac{z}{11.73} + 5.133] \tag{1b}$$

$$\beta(z) = 0.106 + 0.118 \sin[\frac{z}{11.28} + 5.142] \tag{1c}$$

For, $z > 34$m,

$$r_d = 0.12 \exp(0.22M) \tag{1d}$$

According to the equation shown above, z represents the depth below the surface of the Earth in meters, and M represents the magnitude of the earthquake.

Step 4:

Following the Equation (2), the cyclic stress ratio that was induced by the seismic event was calculated as follows:

$$CSR = 0.65 \times \frac{a_{max}}{g} \times \frac{\sigma_v}{\sigma_v'} \times r_d \tag{2}$$

Where, a_{max} is the PGA, and g is the gravitational acceleration.

Step 5:

After a few adjustments, the field SPT-N value is now used to calculate the modified normalized SPT blow number $N_{1,60}$ (Equation 3a).

$$N_{1,60} = CN \times N_{60} \tag{3a}$$

The stress normalizing factor CN is obtained using an empirical formula (Equation 3b). Liao and Whitman [31] proposed a straightforward analytical framework for potential application:

$$CN = 9.79 \times \sqrt{\frac{1}{\sigma_v'}} \tag{3b}$$

Step 6:

Youd and Idriss [32] states that the cyclic resistance ratio is assessed using Equation (4).

$$\mathrm{CRR}_{7.5} = \frac{1}{34-(\mathrm{N}_1)_{60}} + \frac{(\mathrm{N}_1)_{60}}{135} + \frac{50}{10*(\mathrm{N}_1)_{60}-45} - \frac{1}{200} \quad (4)$$

Step 7:

The preliminary liquefaction FS is calculated as follows (Equation 5):

$$\mathrm{FS} = \frac{\mathrm{CRR}_{7.5}}{\mathrm{CSR}} \times \mathrm{MSF} \quad (5)$$

Where, $\mathrm{CRR}_{7.5}$ denotes the cyclic resistance ratio for earthquakes having a moment magnitude (M_w) of 7.5. A correction factor known as the magnitude scaling factor (MSF) is used for earthquakes with magnitudes less or over 7.5. Equation (6), proposed by Youd and Idriss [32], is used for calculating the MSF.

$$\mathrm{MSF} = \frac{10^{2.24}}{\mathrm{M}_{\mathrm{w}}^{2.56}} \quad (6)$$

Where, M_w denotes seismic magnitude.

Step 8:

Utilizing the provided formulae for factor of safety (FS) and liquefaction potential index (LPI), Luna and Frost [26] evaluate the severity of liquefaction by the following expression (Equation 7a-c).

$$\mathrm{LPI} = \sum_{\mathrm{i}=1}^{\mathrm{n}} \mathrm{w_i F_i H_i} \quad (7a)$$

$$\text{Here, } \mathrm{F_i} = 1 - \mathrm{FS_i} \text{ for } \mathrm{FS_i} < 1.0 \quad (7b)$$

$$\mathrm{F_i} = 0 \text{ for } \mathrm{FS_i} \geq 1.0 \quad (7c)$$

Where H_i denotes the thickness of the discretised soil layers; n represents the number of layers; F_i indicates the liquefaction severity for the i-th layer; FSi signifies the factor of safety for the i-th layer; w_i is the weighting factor (=10 – 0.5 z_i); and z_i refers to the depth of the i-th layer (m). The liquefaction classes according to the Liquefaction Potential Index (LPI) are shown in Table 1 below.

Table 1 Liquefaction Severity Level

LPI	Iwasaki et al. [27]	Luna and Frost [26]
0	Very low liquefiable	Effect: none
0 < LPI < 5	Low liquefiable	Effect: Minor
5 < LPI < 15	High liquefiable	Effect: Moderate
15 < LPI	Very high liquefiable	Effect: Major

4.0 SOIL DISTRIBUTION MAP

The design of the structure heavily relies on the geotechnical analysis. Understanding the sub surface's condition is crucial. For the sake of planning and design, a site investigation report is produced. It classifies soil conditions below ground using the results of the hydrometer and sieve analyses. Soil may be classified into three basic types: clay, silt, and sand. But most soils are a combination of many types. The Unified Soil Classification System (USCS) divides fine-grained soils into many categories, such as SM (Silty Sand), CL (Clay with Low Plasticity), CH (Clay with High Plasticity), MH (Silt with High Plasticity), ML (Silt with Low Plasticity), and SC (Clayey Sand). Using the USCS, soil distribution maps are created at different depths. Using ArcGIS software, the distribution of soil type maps at different depths is produced for Dinajpur Municipality (Figures 4-7).

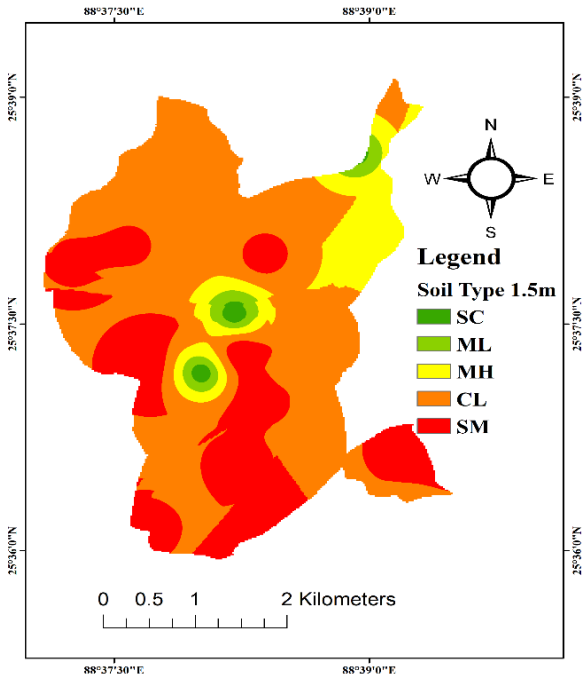


Figure 4 USCS soil classification map at 1.5m depth

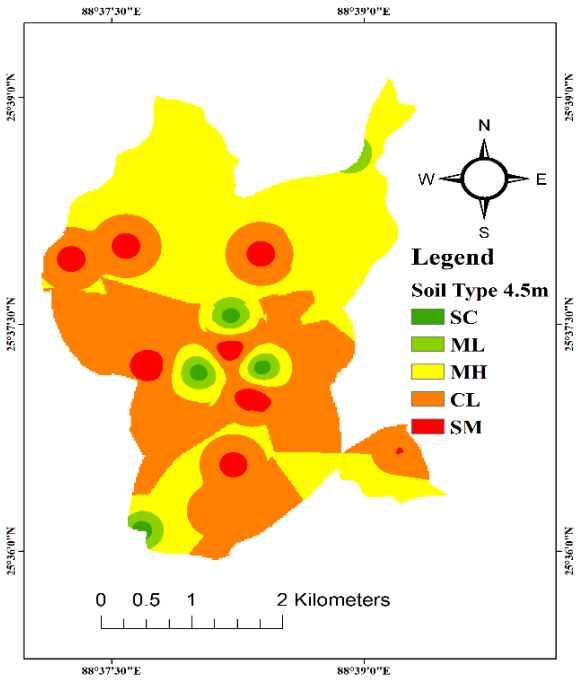


Figure 5 USCS soil classification map at 4.5 m depth

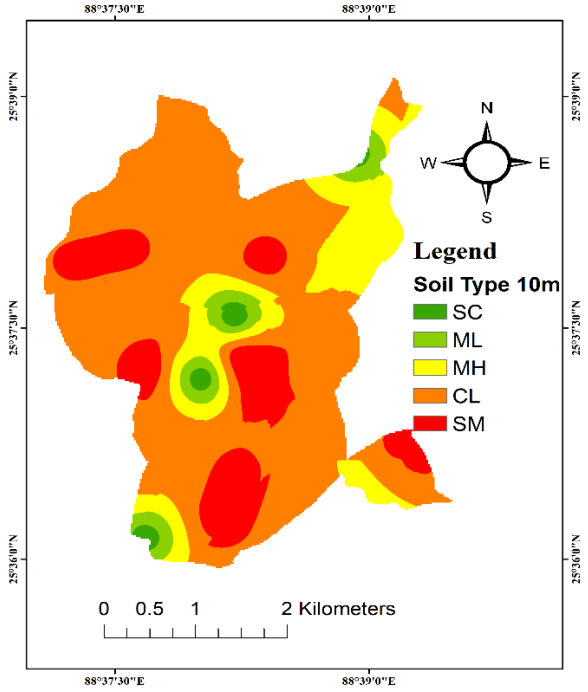


Figure 6 USCS soil classification map at 10 m depth

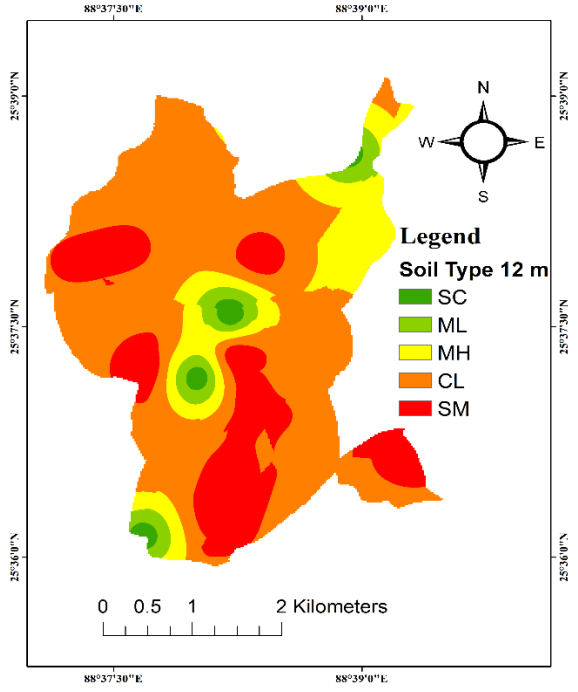


Figure 7 USCS soil classification map at 12 m depth

Soil grading is conducted with the data from 78 boreholes in this region. The USCS categorises soil types as SM, CL, MH, ML, and SC. In Figure 4, the SM and CL soil types mostly encompass Dinajpur Municipality to a depth of 1.5 metres. The soil classifications SC, ML, and MH include a segment of the north-eastern and central regions. Figures 6 and 7 illustrate that changes in soil types are similar. The SC and ML soil types between 4.5 m and 10 m occupy a limited area within the study zone. Figure 5 illustrates that MH soil types mostly occupy the region at a depth of 4.5 metres. At depths of 10 and 12 metres, the SM and CL soil types occupy the most area inside the study zone.

5.0 LIQUEFACTION HAZARD MAP

The factor of safety against liquefaction was assessed using the most current and commonly used empirical methods grounded on field exploration data. The susceptibility of the entire soil layer was determined by integrating the computed FS. The LPI denotes the liquefaction of an entire stratum from the ground surface to a specified depth. A basic Microsoft Excel spreadsheet was developed to compute the LPI of the chosen research area. All boreholes in the study area were effectively used for LPI calculations corresponding to M_w values of 6, 6.5, 7, 7.5, 8, and 8.5. Nonetheless, the LPI assessments for each drill site may not accurately reflect the whole vulnerability of Dinajpur Municipality. The Kriging interpolation method was used to generate risk maps illustrating the actual liquefaction susceptibility inside Dinajpur Municipality. Figures 8–13 depict the LPI distribution for the chosen study area using a streamlined methodology. Although the liquefaction susceptibility is significantly pronounced when LPI exceeds 15.0, the legends provide further colour bars to explain the liquefaction phenomena more effectively. The factor of safety against liquefaction for a moment magnitude of 6 in Dinajpur Municipality has been analysed over many strata using the previously mentioned methodology, including the projected peak ground acceleration, soil properties, and other variables. Figure 8 illustrates the hazard map, indicating that much of the district exhibits significant resistance to liquefaction at low earthquake magnitudes. The majority of the territory is categorised as "very low liquefiable", while a little section is designated as "low liquefiable" in accordance with LPI criteria. The liquefaction vulnerability shown in Figure 9 is derived from an analysis of liquefaction susceptibility, specifically for earthquake magnitudes above $M_w = 6.5$.

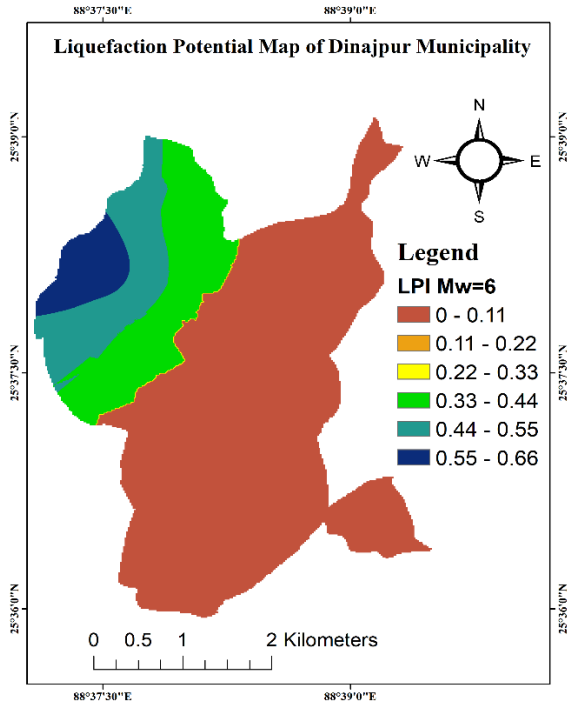


Figure 8 LPI map using IDW interpolation for $M_w = 6$

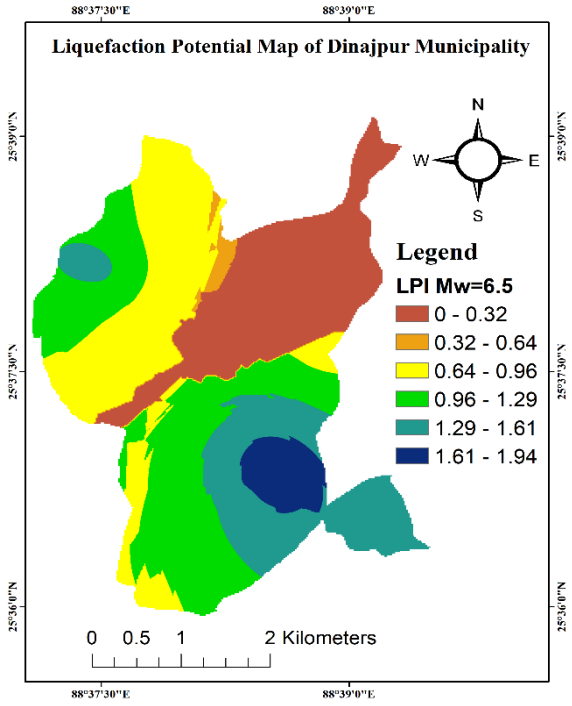


Figure 9 LPI map using IDW interpolation for $M_w = 6.5$

Aside from areas with limited liquefaction potential, the graphic distinctly demonstrates that the north-eastern section of the region is not susceptible to liquefaction after an earthquake of magnitude $M_w = 6.5$. The legend bar indicates that the LPI value varies between 0 and 1.94, with the exception of a small segment of Dinajpur Municipality. Consequently, the legend bar displays a distinct colour. Figure 10 illustrates the impact of a moderate earthquake magnitude. The LPI for $M_w = 7$ ranges from 1 to 5, indicating a "low liquefiable" zone. The majority is classified as "low-liquefiable", while a minor segment is classified as "high-liquefiable", in accordance with LPI. With $M_w = 7.5$, the susceptibility to liquefaction increases correspondingly. Figure 11 illustrates the liquefaction susceptibility map with a moment magnitude of 7.5. The fluctuations in the LPI values were shown using various colours. Except for a minor section deemed "highly liquefiable", most of the region is classified as "low liquefiable" according to LPI criteria.

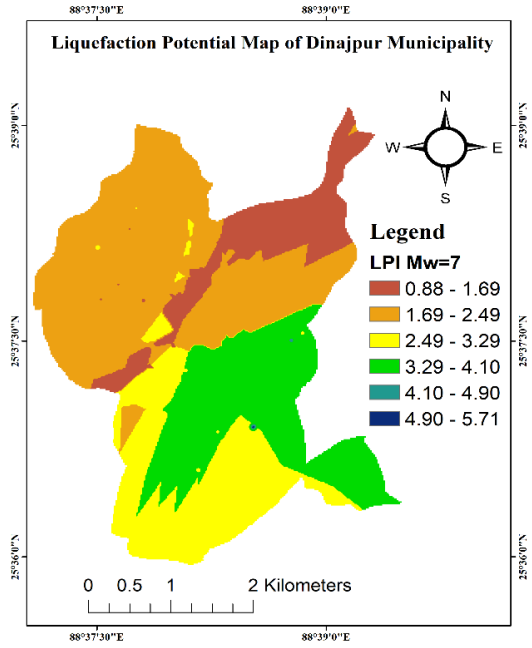


Figure 10 LPI map using IDW interpolation for M_w=7

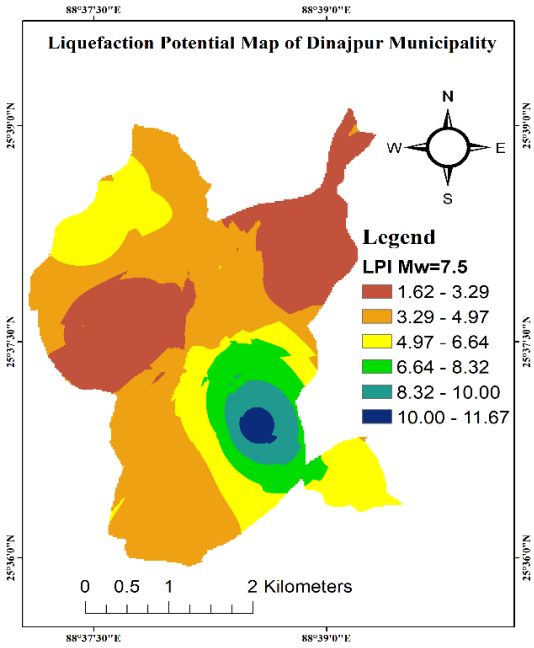


Figure 11 LPI map using IDW interpolation for M_w=7.5

The figure indicates that areas formerly classified as "non-liquefiable" are now categorised as "liquefiable" with an earthquake magnitude of M_w = 8. Figure 12 illustrates the liquefaction hazard map for M_w = 8. The legend bar indicates that the LPI value exceeds five (LPI > 5), with the exception of a small section of the study area, which signifies a low-liquefiable zone. The regions are most susceptible to liquefaction, as indicated on the map, due to an earthquake magnitude of M_w = 8.5. Some regions of the Dinajpur Municipality remain stable owing to soil integrity. Figure 13 illustrates the liquefaction hazard map for a magnitude 8.5 earthquake in the study area.

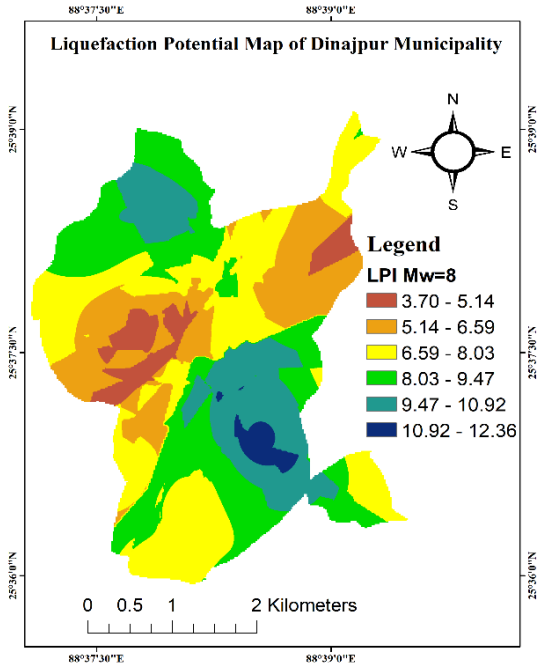


Figure 12 LPI map using IDW interpolation for M_w=8

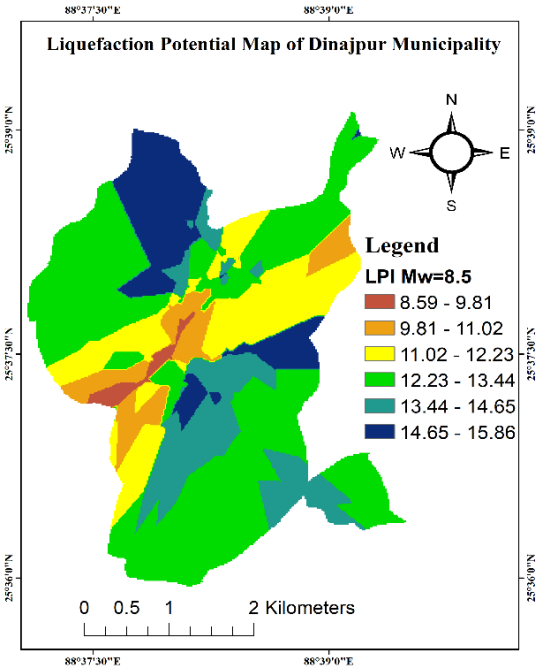


Figure 13 LPI map using IDW interpolation for M_w=8.5

The effects of a major earthquake were depicted in detail on the liquefaction risk map. The majority of formerly "low liquefiable" areas become significantly liquefiable at an earthquake magnitude of M_w = 8.5. With the exception of a little portion of the study region, the legend bar shows that the LPI value varied from 5 to 15, suggesting a very

highly liquefiable zone (LPI>15). Additionally, the legend bar shows that, except for a little portion of the study zone, the LPI value ranges from 10 to 15.9. The LPI classifies a larger fraction as "highly liquefiable", whereas a small portion is classified as "very highly liquefiable."

6.0 CONCLUSIONS

The research project aimed to produce risk maps and soil distribution maps for various soil layers in Bangladesh's Dinajpur Mumwnicipality due to uncertainty in the liquefaction assessment method. The FS of the chosen locations was estimated using a realistic method. After adding up the FS for a particular site, the severity of the liquidation was evaluated at each distinct place. Using Kriging interpolation and geospatial analysis, a liquefaction hazard map was created for the whole study area. It was discovered that the majority of the study area was extremely susceptible to liquefaction at high earthquake magnitudes. Nonetheless, it was determined that the core Dinajpur Municipality was secure from liquefaction. It was discovered that the study area's north and southwest sides were very liquefied. Planners, developers, and geotechnical engineers can use the prepared maps to learn more about Dinajpur Municipality. The liquefaction hazard scenario that was constructed might serve as a helpful indicator for the disaster mitigation plan. However, before the current technique can be included in the code of practice and catastrophic recommendations, a more thorough investigation is required to confirm it.

Conflicts of Interest

None of the contributors have any conflicts of interest.

Acknowledgement

The investigators would like to express gratitude to the LGED and PWD in Dinajpur, Bangladesh for providing sufficient data for this study.

References

[1] Rahman, M. A., Ahmed, S., & Imam, M. O. (2020). Rational way of estimating liquefaction severity: an implication for Chattogram, the Port City of Bangladesh. Geotechnical and Geological Engineering, 38(2), 2359-2375. https://doi.org/10.1007/s10706-019-01134-2

[2] Rahman, M. M., Hossain, M. B., & Sayed, A. (2025). Prediction of soil liquefaction using machine learning approaches. Engineering Transactions, 73(2), 1-22. https://doi.org/10.24423/engtrans.3360.2025

[3] Sayed, A., & Rahman, M. M. (2025). M5 soft computing techniques for assessment of soil liquefaction. Journal of Rehabilitation in Civil Engineering, 13(3), 199-214. https://doi.org/10.22075/jrce.2025.34669.2134

[4] Bilham, R., & England, P. (2001). Plateau 'pop-up' in the great 1897 Assam earthquake. Nature, 410(6830), 806-809. https://doi.org/10.1038/35071057

[5] Hossain, M. B., Rahman, M. M., & Haque, M. R. (2021). Empirical correlation between shear wave velocity (Vs) and uncorrected standard penetration resistance (SPT-N) for Dinajpur District, Bangladesh. Journal of Nature, 3, 25-29. https://doi.org/10.36937/janset.2021.003.005

[6] Mostazid, M. I., Mahabub, M., & Mahbur, M. (2019). Seismic vulnerability assessment of existing RCC buildings in Dinajpur City: a case study on ward no 6. In 2nd International Conference on Planning, Architecture & Civil Engineering, 1-6.

[7] Ministry of Disaster Management and Relief. (2015). Atlas: Seismic risk assessment in Bangladesh for Bogra, Dinajpur, Mymensingh, Rajshahi, Rangpur and Tangail City Corporation / Paurashava Areas, Bangladesh.

[8] Mayya, A., Zenab, A. A., & Chatterjee, K. (2025). Evaluation of liquefaction potential of Kolkata City, India, using LPI and LSN approaches. Indian Geotechnical Journal, 55(2), 652-668. https://doi.org/10.1007/s40098-024-01002-8

[9] Singh, M. (2024). Liquefaction hazard analysis of Varanasi city of Northern India. Natural Hazards, 120(6), 4985-5005. https://doi.org/10.1007/s11069-024-06417-3

[10] Kumar, S., Muley, P., & Syed, N. M. (2023). Soil liquefaction potential of Kalyani region, India. Indian Geotechnical Journal, 53(1), 139-153. https://doi.org/10.1007/s40098-022-00658-4

[11] Hossain, A. T. M. S., Mahabub, M. S., Dutta, T., Khatun, M., Terao, T., Imam, M. H., & Jafrin, S. J. (2023). The hidden earthquake induced liquefaction risks in the Rohingya refugee camp hills & surrounding areas of Ukhiya,

Cox's Bazar, Bangladesh—a geotechnical engineering approach. Open Journal of Earthquake Research, 12(3), 114-138. https://doi.org/10.4236/ojer.2023.123004
[12] Ansari, A., Zahoor, F., Rao, K. S., & Jain, A. K. (2022). Liquefaction hazard assessment in a seismically active region of Himalayas using geotechnical and geophysical investigations: a case study of the Jammu Region. Bulletin of Engineering Geology and the Environment, 81(9), 349. https://doi.org/10.1007/s10064-022-02852-3
[13] Subedi, M., & Acharya, I. P. (2022). Liquefaction hazard assessment and ground failure probability analysis in the Kathmandu Valley of Nepal. Geoenvironmental Disasters, 9(1), 1. https://doi.org/10.1186/s40677-021-00203-0
[14] Nath, S. K., Madan, J., & Sharma, S. P. (2025). Surface-consistent seismic hazard and holistic microzonation vis-à-vis socio-economic risk and damage potential studies of Northeast India and Bhutan. Journal of the Geological Society of India, 101(6), 844-849. https://doi.org/10.17491/jgsi/2025/174171
[15] Mase, L. Z., Likitlersuang, S., & Tobita, T. (2022). Verification of liquefaction potential during the strong earthquake at the border of Thailand-Myanmar. Journal of Earthquake Engineering, 26(4), 2023-2050. https://doi.org/10.1080/13632469.2020.1751346
[16] Rahman, M. M., Hossain, M. B., & Roknuzzaman, M. (2023). Effect of peak ground acceleration (PGA) on liquefaction behavior of subsoil: A case study of Dinajpur Sadar Upazilla, Bangladesh. AIP Conference Proceedings, 2713, 030002. https://doi.org/10.1063/5.0129770
[17] Sukkarak, R., Tanapalungkorn, W., Likitlersuang, S., & Ueda, K. (2021). Liquefaction analysis of sandy soil during strong earthquake in Northern Thailand. Soils and Foundations, 61(5), 1302-1318. https://doi.org/10.1016/j.sandf.2021.07.003
[18] Hossain, M.B., Roknuzzaman, M., & Rahman, M. M. (2022). Liquefaction potential evaluation by deterministic and probabilistic approaches. 8(7), 1459-1481. http://dx.doi.org/10.28991/CEJ-2022-08-07-010
[19] Hossain, M. B., & Rahman, M. M. (2025). Seismic microzonation and probability of ground failure assessment caused by liquefaction for Bogura District, Bangladesh. Journal of Rehabilitation in Civil Engineering, 13(2), 218-242. http://dx.doi.org/10.22075/jrce.2024.34111.2086
[20] Tint, Z. L., Kyaw, N. M., & Kyaw, K. (2018). Development of soil distribution and liquefaction potential maps for downtown area in Yangon, Myanmar. Civil Engineering Journal, 4(3), 689-701. https://doi.org/10.28991/cej-0309108
[21] Rahman, M. M., Hossain, M.B., Sayed, A., & Thakur, S. (2024). Assessment of liquefaction potential based on the logistic regression machine learning algorithm. In 7th International Conference on Civil Engineering for Sustainable Development (ICCESD 2024), Bangladesh
[22] Kayal, J. R., Arefiev, S. S., Baruah, S., Hazarika, D., Gogoi, N., Gautam, J. L., & Tatevossian, R. (2012). Large and great earthquakes in the Shillong plateau–Assam valley area of Northeast India Region: Pop-up and transverse tectonics. Tectonophysics, 532, 186-192. https://doi.org/10.1016/j.tecto .2012.02.007
[23] Rahman, M. M., & Sarder M., (2026). GIS-based semi-variogram model selection for the preparation of Modified Mercalli Intensity map of Dinajpur Sadar, Bangladesh. International Journal of Engineering and Geosciences, 11(1), 136-148. https://doi.org/10.26833/ijeg.1656666
[24] BNBC. (2015). Bangladesh National Building Code.
[25] Steckler, M. S., Akhter, S. H., & Seeber, L. (2008). Collision of the Ganges–Brahmaputra delta with the Burma Arc: Implications for earthquake hazard. Earth and Planetary Science Letters, 273(3-4), 367-378. https://doi.org/10.1016/j.epsl.2008.07.009
[26] Luna, R., & Frost, J. D. (1998). Spatial liquefaction analysis system. Journal of Computing in Civil Engineering, 12(1), 48-56. https://doi.org/10.1061/(ASCE)08873801(1998)12:1(48)
[27] Iwasaki, T., Tokida, K. I., Tatsuoka, F., Watanabe, S., Yasuda, S., & Sato, H. (1982, June). Microzonation for soil liquefaction potential using simplified methods. In Proceedings of the 3rd international conference on microzonation, Seattle, 3(2), 1310-1330
[28] Youd, T. L., & Idriss, I. M. (1997). Proceeding of the NCEER workshop on evaluation of liquefaction resistance of soils. In Proceeding of the NCEER workshop on evaluation of liquefaction resistance of soils (pp. 276-276).
[29] BNBC. (2020). Bangladesh National Building Code.
[30] Idriss IM, Boulanger RW (2006) Semi-empirical procedures for evaluating liquefaction potential during earthquakes. Soil Dyn Earthq Eng 26:115–130. https://doi.org/10.1016/j.soildyn.2004.11.023
[31] Liao, S. S., & Whitman, R. V. (1986). Overburden correction factors for SPT in sand. Journal of geotechnical engineering, 112(3), 373-377. https://doi.org/10.1061/(ASCE)07339410(1986)112:3(373)
[32] Youd, T. L., & Idriss, I. M. (2001). Liquefaction resistance of soils: summary report from the 1996 NCEER and 1998 NCEER/NSF workshops on evaluation of liquefaction resistance of soils. Journal of geotechnical and geoenvironmental engineering, 127(4), 297-313. https://doi.org/10.1061/ (ASCE) 10900241(2001)127: 10(817)